



EXPERIMENTAL INVESTIGATION OF STRENGTHENING OF NON DUCTILE RC BEAMS USING FRP

C.A. Zeris¹

ABSTRACT

An experimental investigation is presented comparing the response of four full size reinforced concrete (RC) beams, mostly without current detailing provisions for ductility, typical of existing RC buildings designed with past seismic regulations. All specimens are initially strengthened with synthetic fiber reinforced polymers (FRP) and are tested as continuous two-span beams with different shear span to depth ratios, their response being compared to a control specimen encompassing currently enforced detailing provisions. Three alternative strengthening methods are considered. The tests demonstrate that specimens with longitudinal side strengthening exhibit a larger ductility capacity, compared to the specimen strengthened with conventional top and bottom FRP application. Furthermore, the reliability of current design analytical models for strength prediction is evaluated, considering their ability to predict experimental behavior.

Introduction

In current seismic design, equivalent seismic design loads are reduced making use of the fact that the entire RC structure and its constitutive elements possess adequate energy absorption capacity and ductility supply in their critical regions. Let alone reasons of economy, provision of ductility and hysteretic absorption supply in RC building performance is deemed essential due to the fact that the intensity level and damage potential of the base excitation cannot be quantified yet with sufficient reliability, nor is the nonlinear time-varying nature of the response similar to the simplified equivalent linear elastic methods employed for seismic design. The influence of these uncertainties to structural performance increases particularly when dealing with members in existing RC structures, which are designed with past seismic codes, which tend to fail in a brittle mode in shear and have no capacity for ductility and strength redistribution.

The experimental behavior of one control and three test elements are presented herein, tested monotonically after having been strengthened using three alternative methods of FRP application adopted in practice with different types of FRP materials. All the specimens are full scale, tested as two-span continuous beams. The objective of the tests is to investigate the ability

¹Lecturer, Dept. of Civil Engineering, National Technical University of Athens. Zografou, GR 15773, Greece.
zeris@central.ntua.gr

of existing RC beams with a low shear span to depth (a/d) ratio and poor transverse reinforcement details, characteristic of existing non conforming buildings designed to older seismic provisions, to be strengthened with FRP so as to exhibit a ductile flexural response comparable to those of a contemporary conforming structure.

The contribution of FRP to shear strengthening of beams has been analyzed in several recent comprehensive literature reviews and parametric investigations (ACI Committee 440, 2000; FIB-TG 9.3, 2001; Triantafillou and Antonopoulos 2000; Bonacci and Maalej 2001; and Bouselham and Chaallal 2004). Furthermore, the verification of shear strengthening models using FRP, the critical parameters and the FRP application technology have been studied experimentally mostly under monotonic testing. Tests have been performed on rectangular beams with a/d of 3.0 by Bencardino et al. (2002) and Pellegrino and Modena (2002), who proposed an upper bound of U or side applied shear contribution of the FRP, in terms of the ratio of transverse rigidity of conventional steel stirrups and FRP reinforcement. Furthermore, Alagusundaramoorthy et al. (2003) tested fourteen rectangular beams with a/d of 5.40. Grace et al. (2002; 2003) tested in all twenty rectangular simply supported beams with a/d of 3.60, in order to verify different FRP sheet properties. Micelli et al. (2002) tested statically twelve RC T joists from an existing decommissioned building with a/d equal to 2.50, yielding an overestimation of the shear strength by 200% to 800% of the conventional strut and tie predictions due to premature peeling of the strengthening materials. In fact, the extension of the conventional strut and tie approach to FRP shear strengthening design has been questioned by several investigations (Stratford and Burgoyne 2003; Vougioukas et al. 2005).

Although the cyclic response of columns and bridge piers has been investigated under lateral load reversals, generally, cyclic testing in beams has not been equally investigated, even though FRP materials are increasingly being used for strengthening of this type of elements. Following the recent damaging earthquakes in Greece, there has been an increasing use of FRPs (primarily as unidirectional sheets of glass – GFRP – or carbon – CFRP – fibers) for the repair and/or strengthening of existing RC buildings. Such buildings have been designed following past seismic provisions without full compliance to currently adopted detailing and analysis requirements for ductile seismic performance. Consequently, their structural members are generally characterized by inadequate stirrup layout and spacing, due to the absence of any capacity design and confinement detail requirements during the time their design was effected.

In order to investigate the reliability of the design models and the performance of existing RC members retrofitted and/or strengthened using FRP materials under seismic type of loading, a series of tests have been performed at the RC Laboratory of the National Technical University of Athens. The tests, all in full size elements, included: a) columns of square or rectangular cross section, tested under constant axial load to failure, subsequently retrofitted and/or strengthened with FRP and retested under similar conditions and b) continuous rectangular two-span beams strengthened using FRP materials in different ways of application and tested to failure, under monotonic or cyclic load reversals of similar form.

Description of the Test Specimens

Layout, Design and Reinforcement Details of the Specimens

Due to space limitations, only the results of the monotonic tests, in the latter group of beam specimens, are presented herein. The design predicted and the experimentally obtained

shear force capacity of the specimens are compared and the observed form of failure is discussed. Complete details of the test sequence, specimen design and both cyclic and monotonic test results are described with the column tests, in the Final report of this project (Zeris 2004).

Test Setup. Four pairs of beams were manufactured, having identical longitudinal reinforcement and different transverse stirrup layouts, depending on the code generation considered for the test: in each pair, one specimen is tested under monotonic loading (as described herein) while the next under increasing amplitude cyclic deformation reversals (Zeris, 2004). All specimens were full size two span continuous beams, with a total length of 3.40m (Fig.1(a)). The specimen exterior roller supports (points A and D in Fig. 1(a)) are at 0.125 m from either end. A third internal pinned support is located at B, 1.20 m from point A. The controlled transverse deformation δ is imposed by a transverse load P at the midpoint C of span BD, which is 1.95 m long. The beam is statically indeterminate of the first degree, therefore, the member transforms into a mechanism following the successive formation of two internal flexural hinges: the first hinge will form at point C, followed by a second hinge at support B in opposite bending, thereby creating an internal point of contraflexure in the region BC.

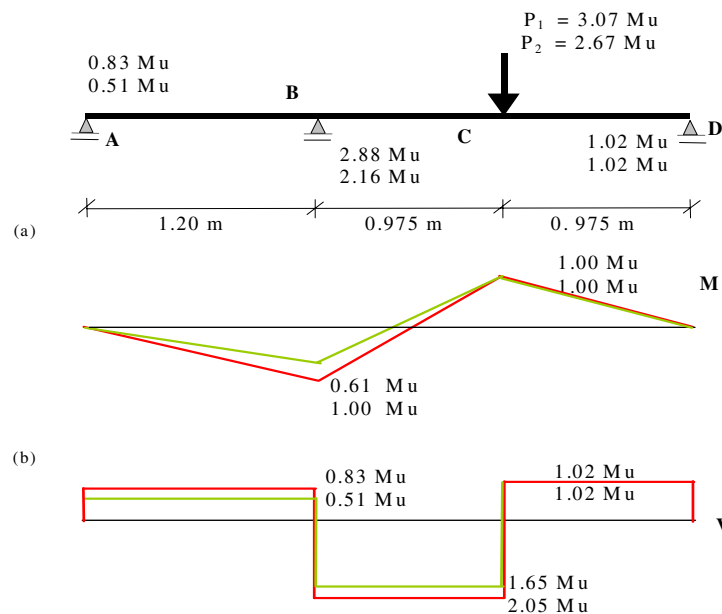


Figure 1. Internal force diagrams of the two-span continuous beams tested, at the formation of the first (green line - top value) and second (red line - bottom value) plastic hinge formation: (a) applied load (P); and (b) moment (M) and shear force (V) diagrams.

Assuming rigid plastic behavior in these two critical sections, the internal force diagrams (bending moment M and shear force V) at the first and second hinge formation are depicted in Fig. 1(b) in terms of the ultimate flexural resistance M_u at the critical sections. In this context, the measurement of the member resistance P under imposed deformation yields the flexural resistance at failure in the critical regions as well as the internal peak shear force resisted in the different spans with different a/d ratios. For the case of the strengthened elements exhibiting

significant hardening, the level of flexural resistance in the two hinges is not equal. In this case, therefore, without the use of additional reaction measurements in the interior supports, only an average flexural resistance M_u in the two hinges can be deduced from the measurement of P .

Description of the Specimens. All beams were 200 mm by 400 mm rectangular in cross section, reinforced longitudinally with three mild steel bars at top and bottom, 14 mm in diameter (Fig. 2). Transverse reinforcement varies depending on the specimen type as follows.

1) Of the four pairs, the first – namely the control group DRC - is detailed with closely spaced closed stirrups over their entire length, in accordance with currently established seismic detailing provisions. Critical region confinement is specified throughout the length using 8 mm diameter high strength stirrups at 100 mm spacing having a closed 145° hook. The specimens in this group received no further strengthening, yet they served to provide the actual ‘as built’ flexural capacity of the test beams, as well as the seismic performance indices of this form of test specimen, namely ductility, overstrength, maximum shear resistance and form of failure.

The other three pairs were all similarly reinforced longitudinally, subsequently receiving FRP strengthening as depicted in Fig. 2. In all these beams the transverse reinforcement consisted of overlapping mild steel stirrups 8 mm in diameter, positioned at 200 mm o/c at regions AB and CD, in order to satisfy minimum spacing requirements and at 100 mm o/c at region BC, following an allowable stress design approach. These specimens were subsequently strengthened as follows:

2) Beams CFS (Fig. 2(a)) were strengthened in flexure applying longitudinally one CFRP sheet 200mm wide, positioned in the conventional manner at the top and bottom faces of the beam, over their entire length.

3) Beams GFS (Fig. 2(b)) were strengthened in flexure by applying three longitudinal sheets of GFRP at each side face of the beam, 400 mm wide, acting in the longitudinal beam direction along their entire length.

4) Finally, beams CFR were strengthened in flexure using a total of eight CFRP rods. These were positioned in four pairs of grooves, 30 mm wide by 25 mm deep, preformed at the cover concrete, in each face, 50 mm from the top and bottom faces and to each other (Fig. 2(c)).

Strengthening Design. In order to account for the increase in flexural resistance in these three groups, all six specimens above were subsequently strengthened in shear with fully wrapped transverse GFRP sheets, either continuous or in the form of strips. The amount of shear strengthening was estimated following a capacity design approach, by way of which the design shear force was 140% higher than the capacity shear determined assuming a fully plastic condition in each of the two hinges: hinge moments were established from plane section analyses, using actual unfactored material properties and assuming that the longitudinal strain at the concrete-FRP interface reached the value of 0.6% in tension prior to failure of the interface.

Following conventional FRP design in shear, the total shear resistance is equal to additive contributions from FRP, conventional stirrups and the concrete mechanisms (friction, dowel and aggregate interlock). The contribution of the transverse FRP in shear resistance was estimated from the conventional truss analogue model (e.g. Eqs. 10-3 to 10-5 in ACI Committee 440 (2000)), with the added conservatism on this side of the design equation, that the effective strain in the FRP laminates (ϵ_{fe}) was equal to the yield strain of the conventional transverse steel acting in parallel with the FRP which was experimentally determined to be 0.18%. Furthermore, in accordance with current seismic design regulations in Greece for RC beams, only 30% of the additive concrete contribution to shear resistance was included in the transverse FRP design.

Therefore, the effective strain of the FRP assumed in the design is smaller than the conventional value obtained after imposing all relevant strength reduction factors to the effective FRP strain of 0.40% suggested for fully wrapped members in Section 10.4.1 of ACI Committee 440 (2000). It is also lower than the value suggested by Triantafillou and Antonopoulos (2000), obtained from a statistical evaluation of experimental effective strain limits in shear from a wider database of tests. As also mentioned earlier, the use of the above additive law for different resisting mechanisms in FRP shear design, some of which are brittle in nature and interact with each other, has been questioned (Stratford and Burgoyne 2003; Vougioukas et al. 2005); nevertheless, it has been adopted herein, being subject to investigation.

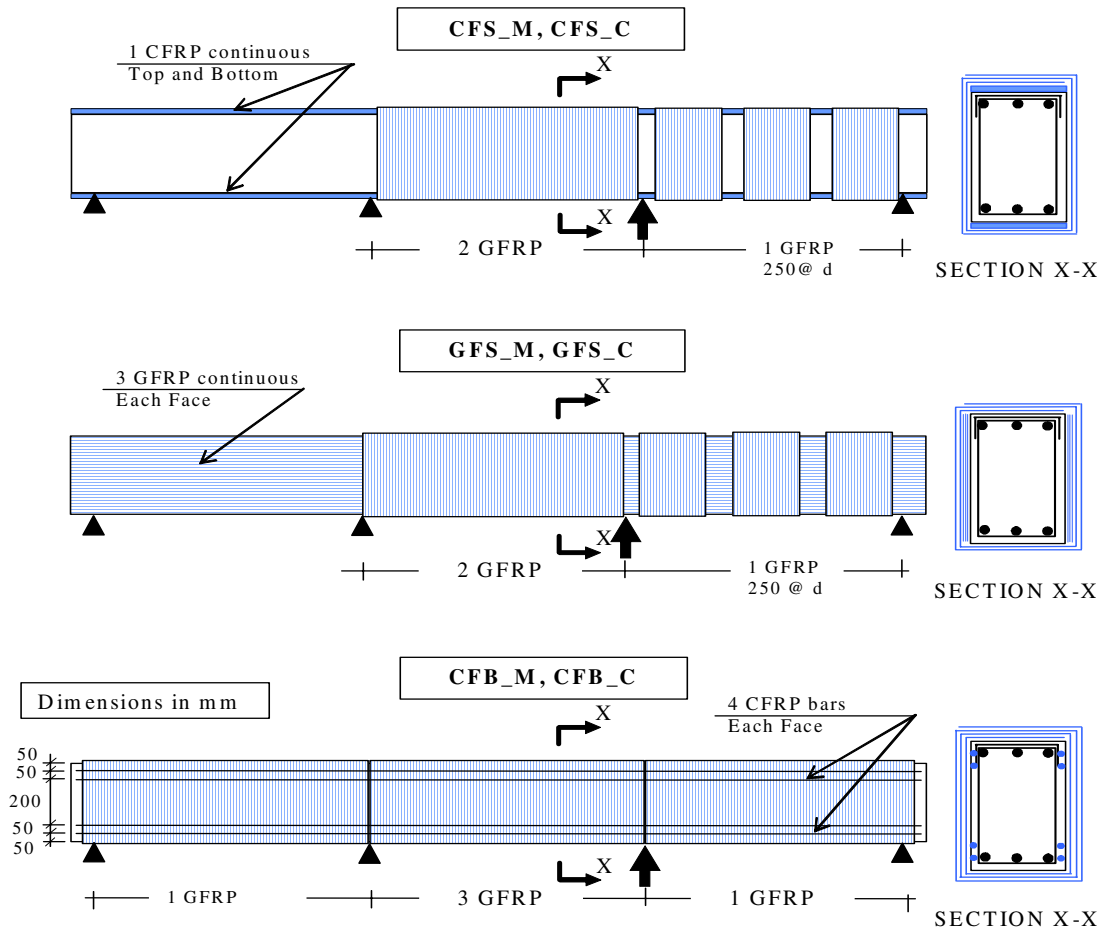


Figure 2. FRP sheet or rod reinforcing details for the six strengthened specimens.

According to the test program, of the eight beams manufactured as described, four were tested under monotonic loading (discussed herein) and four under cyclic loading (Zeris 2004). In all cases of FRP sheet application, the wet lay up method was adopted. Beam surfaces were smoothed with a grinder at the top casting surface and all surface defects due to casting were patched with non-shrink grout. All the section edges were rounded at the four corners to a specified radius of curvature with a disk grinder and subsequently the member was cleaned with compressed air and its surfaces to receive FRP were treated with a two-component primer that sealed all the pores of the concrete surfaces. After the primer was allowed to set for twenty four hours, the FRP sheets were fixed to the concrete surface with a two-component epoxy resin,

using hand application and a steel roller to remove all entrapped air bubbles. CFRP rods were hand pushed into the grooves at the side faces, trowel filled with a non shrink epoxy cementitious grout and subsequently covered with this grout up to the surface. The surface was also trowel finished, in order to apply the transverse strengthening reinforcement.

Structural Material Characteristics_. Three different types of steel were used for conventional reinforcement, with the following average mechanical characteristics: 14mm diameter smooth longitudinal reinforcement for flexure, with 365 MPa yield and 460 MPa ultimate tensile strength; 8mm diameter mild steel stirrups (smooth) for transverse reinforcement of the three test groups to receive FRP strengthening (Groups CFS, CFR and GFS), with 370 MPa yield and 520 MPa ultimate tensile strength; and, finally, 8mm diameter ribbed high strength reinforcement, for the transverse reinforcement of the control (DRC) Group elements, with 605 MPa yield and 673 MPa ultimate tensile strength.

For the FRP sheets nominal properties were assumed in design, respectively, as provided by the manufacturer specification (Mac Beton, 2002): a) GFRP sheets have a thickness of 0.23 mm, a modulus of elasticity of 65,000 MPa and a maximum strength and fracture strain of 1,700 MPa and 2.60%, respectively; b) CFRP sheets have a thickness of 0.165 mm, a modulus of elasticity of 230,000 MPa and a maximum strength and corresponding fracture strain of 3,450 MPa and 1.50%, respectively; c) finally, the CFRP rods were 7.5mm in diameter with a quartz sand surface finish. They exhibit a modulus of elasticity of 130,000 MPa and a maximum strength and corresponding fracture strain of 2,300 MPa and 1.80%, respectively. Concrete used was grade C20 ready mix having a specified characteristic cylinder strength of 20 MPa (namely only 5% of the specimens expected to fall below this value). From tests on cylinders obtained after casting, just before the time of testing, the average uniaxial cylinder compressive strength of the concrete was established to be equal to 26.7 MPa, with a standard deviation of 2 MPa.

Experimental Results

All tests were conducted under transverse deformation control. In addition to the member resistance at the load application point, longitudinal strains were measured with 3cm strain gauges at the longitudinal reinforcement location, while transverse strains were also monitored using two 10cm strain gauges, positioned on the transverse FRP surface at the midheight of the beams, at $d/4$ intervals away from the load point and towards the interior support (where d is the effective beam depth). The measured load deformation characteristics are presented in Figures 3 and 4, with a discussion of the form of failure obtained in each case, followed by a photograph of the specimen at the end of the test, after the FRP sheets have been removed.

In Table 1 are provided the key recorded performance characteristics of the experimental response. These include the resistance at incipient yielding of the conventional tension steel in the first hinge location P_{1y} and corresponding deformation δ_y , the maximum resistance P_u , the member overstrength Ω ($= P_u/P_{1y}$), the usable deformation δ_{u85} , corresponding to the deformation at which the resistance drops below 85% P_u and the maximum deformation of the test δ_{max} . The recorded behavior is also approximated by an equal area elastoplastic bilinear approximation, having an initial linear part passing through the resistance value of 0.60 P_u , and a maximum deformability at δ_{u85} , exhibiting an equivalent yield displacement $\bar{\delta}_y$. The ratios of δ_{u85} to δ_y or $\bar{\delta}_y$ define the global ductility capacity ratios of the specimen, also quoted in Table 1.

The corresponding predicted parameters include the theoretical resistance values P of the elastoplastic beam of Fig.1, adopting corresponding limit state bending moments at the hinge locations; in this context, the resistance at incipient tensile steel yield, P_{ly} , corresponds to the first plastic hinge moment set equal to M_y (tensile steel strain equal to 0.18%, Table 1); furthermore, for the strengthened specimens, the theoretical resistance levels $P_{2u0.6}$, $P_{2u0.8}$ and $P_{2u1.1}$ are also calculated (where $P = 3.07 M$ from Fig.1), corresponding to the formation of two hinges with flexural resistance at peak effective FRP tensile strains of 0.6% and 0.8% and 1.1% respectively. All the above values were estimated using a plane sections remain plane analysis program by Chadwell and Mahin (2000), in which measured unfactored characteristics for steel and concrete and nominal properties for the FRP materials, were specified.

Table 1. Predicted and measured performance characteristics.

		DRC	GFS	CFS	CFR
Predicted	M_y , kNm	57.2	64.2	59.7	67.2
	P_{ly} , kN	152.7	171.4	159.4	179.4
	$P_{2u0.6}$ kN ($\epsilon_{fe} =$	215.8	253.9	230.6	291.7
	$P_{2u0.8}$ kN ($\epsilon_{fe} =$		273.2	247.7	330.9
	$P_{2u1.1}$ kN ($\epsilon_{fe} =$		313.5	278.5	387.1
Recorded	P_{rv} / P_{m} , kN	154 /	179 /	165.8 /	185.5 / 312.7
	Ω	1.46	1.99	1.63	1.69
	$\delta_y / \bar{\delta}_y$, mm	6.6 / 9.0	8.7 / 17.3	7.2 / 9.9	8.7 / 13.0
	$\delta_{u85} / \delta_{max}$, mm	24.2* /	76 / 85	22 / 74	56 / 110
	$\mu_{\delta} = \delta_{u85} / \delta_y$ or $\bar{\delta}_y$	3.7* / 2.7*	8.7 / 4.4	3.1 / 2.3	6.4 / 4.3

Test DRC behaved in an ideal ductile manner, as expected from a specimen designed to the current codes, despite its low a/d ratio equal to 1.0. Two plastic hinges have been detected, marked by dominant vertical cracks at the load point, first, and subsequently the internal support. Following the formation of the second hinge (at about 175 kN), a hairline diagonal crack at C towards B closed, due to the redistribution of forces (Fig. 3(a)). It should be mentioned at this point that specifically for test DRC, the maximum deformability of the member quoted in Table 1 (marked *) was not fully established since the test was concluded before any serious damage was induced in the member (Fig. 3(a)). Being first in the series, this test also served as a means of calibrating the statically indeterminate test setup by introducing two 300kN load cells in series with the supports at B and D. Their presence allowed for measuring of internal reaction values, comparable to those obtained from the theoretical model, but did not allow for large inelastic rotations to take place at the supports. In any case, the member provided the minimum displacement ductility required by code before this test was concluded (Table 1).

Test CFS exhibited the highest initial lateral stiffness among the three tests (110% of control test DRC), the remaining two specimens depicting comparable stiffness due to the use of more flexible FRP, distributed at the sides. After the formation of the first hinge, longitudinal tensile cracks at the weak direction of the transverse FRP were also obtained at the second hinge location, around 200 kN load, following yielding at this point. The specimen failed abruptly at

270 kN, with a discrete crack formation at C towards the support D due to tensile fracture of the longitudinal CFRP sheet. As a result, a vertical – diagonal crack formed at the web, with interface splitting under the FRP stirrup (Fig. 3b). The test was continued to a maximum deformation of 70mm without the formation of any new significant cracks, with the specimen exhibiting a constant residual resistance of about 220 kN, comparable to the residual strength of specimen DRC. Both transverse strain gauges recorded maximum strains between 0.05‰ and 0.08‰ in the FRP direction. From plane section analyses, the recorded ultimate member strength of 270 kN corresponds to an average longitudinal effective FRP strain of 10‰ at each hinge.

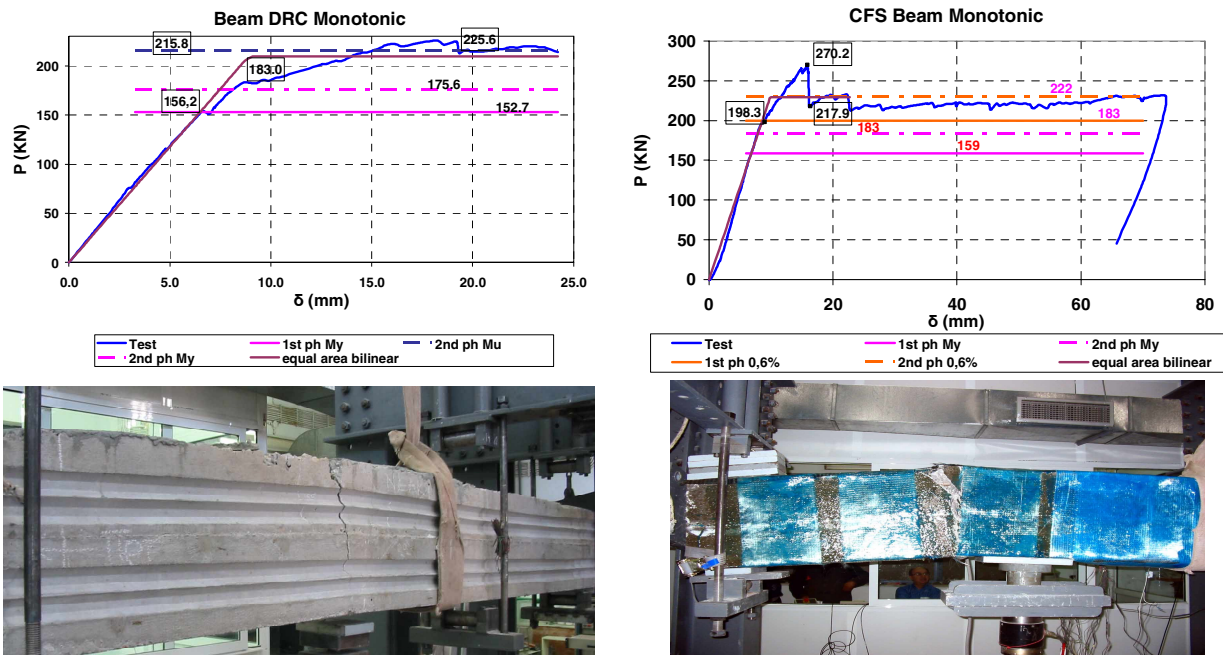


Figure 3. Force deformation diagrams and failure patterns. Specimens: (a) DRC and; (b) CFS.

Contrary to the above, the formation of the first plastic hinge in specimen GFS was marked by a gradual tensile failure of the longitudinal FRPs near the top above the load point. The effective depth of tensile FRP failure contributing to the resistance, increased gradually as the deformation increased, reaching a maximum of about half of the effective depth and spreading on each side of the load. Similar though less marked distress was observed also at the second hinge at the internal support. The specimen did not exhibit a catastrophic failure: after reaching a maximum load of 356.5 kN (corresponding to an average longitudinal effective FRP strain at the extreme fiber of 16‰, in this case), the side FRP gradually failed as a zipper with a consequent gradual reduction in resistance. The residual strength did not fall below 300 kN, or 140% of the DRC residual strength, up to the maximum useable deformation of 76mm (Fig. 4(a)). The test was concluded at 85mm, marked by failure of the FRP-concrete interface in region AB, where no transverse FRP reinforcement was applied due to the small amount of shear demands. The maximum strain recorded in the transverse strain gauges was 3.0 ‰ in the gauge closest to the load point, found to be located over the diagonal crack that marked the failure pattern after exposure of the element (Fig. 4(a)); it should be noted that the second gauge,

located only 10cm away from this crack, recorded insignificant measurements.

Similar post-ultimate behavior was also observed in test CFR, with a slightly more pronounced drop in its resistance after the peak (Fig. 4(b)), compared to GFS, yet without the sudden brittle type loss of resistance of member CFS. The specimen was able to mobilize two plastic hinges and a maximum useable deformation of 56mm and residual strength of 245 kN, up to a deformation of 80mm. Besides the formation of shear-flexural cracks, failure of the CFRP bar anchorage was observed primarily at the first hinge location, where the inelastic rotations concentrated, with consequent destruction of one of the top CFRP bars at the crack intersection (Fig. 4(b)). Both transverse strain gauges recorded similar maximum strains, around 0.65 ‰.

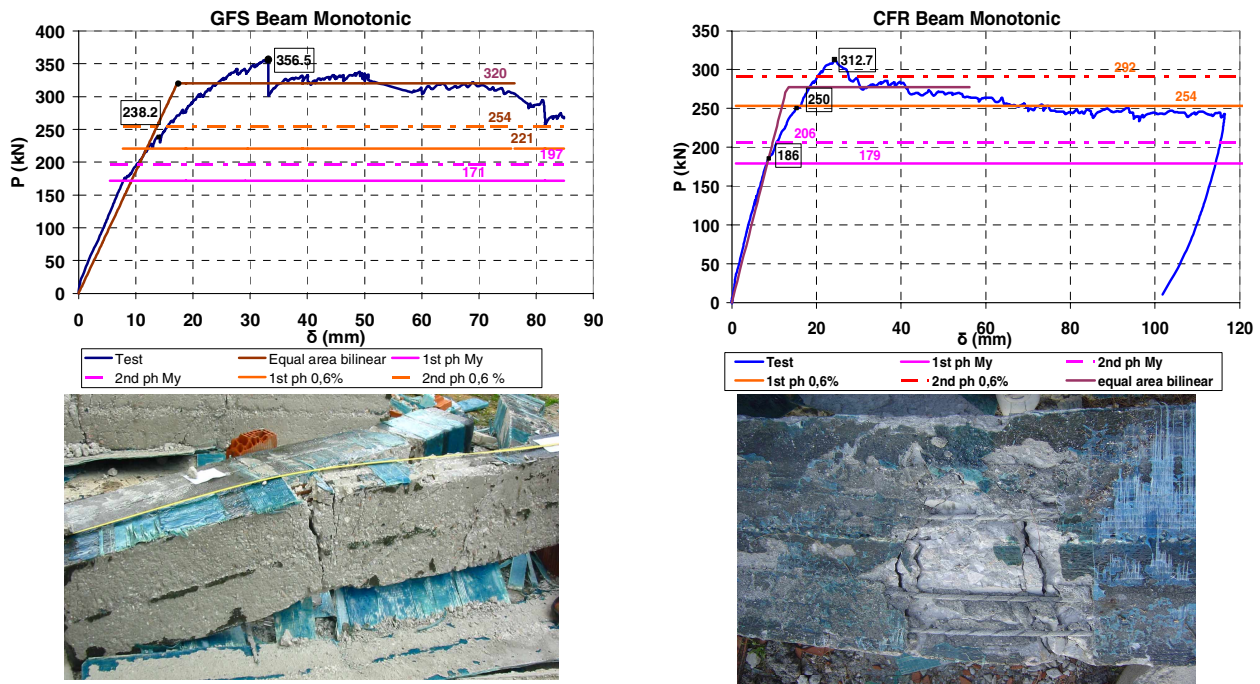


Figure 4. Force deformation diagrams and failure patterns; Specimens (a) GFS; and (b) CFR.

Conclusions

Monotonic tests on two-span continuous beams which had been detailed according to past seismic design detailing regulations and strengthened with three alternative means of FRP application are compared with a similar test of an identical beam, conventionally reinforced following current code requirements for ductile seismic performance.

The control beam which was initially designed for ductile flexural response with closely spaced steel ties exhibited a stable response and high ductility, despite its low a/d ratio of 1.30. All three strengthened specimens were able to develop a full flexural type of collapse mechanism, forming two flexural hinges. The measured shear demands corresponded to effective longitudinal FRP contributions of 1.6% (GFRP sheets at the sides), 1,0% (CFRP at top/bottom) and 0.7% (CFRP rods at the sides), higher than normally adopted for the estimation of the design flexural resistance. Higher FRP strains should therefore be adopted for capacity design.

The effective failure strain measured at the transverse FRP sheets varied with the method of strengthening adopted. Minimum transverse strains were obtained in the top and bottom applied FRP due to failure in a different region, compared to the side strengthened specimens in which the FRP sheets mobilized to a recorded maximum strain of 0.65‰ (specimen CFR) and 3.0‰ (specimen CFS). The mobilization of the FRP in the latter case was highly localized.

Contrary to the conventionally strengthened beam, characterized by abrupt total loss of its overstrength at a deformation of 17mm, the resistance of the side strengthened specimens never dropped below the control member peak resistance up to deformations between 65mm and 85mm (ductilities of 6.0 or 9.0) for the specimen using bars or sheet, respectively. The maximum ductility capacity of the conventionally strengthened specimen was only 3.0, which corresponded to a chord rotation at failure of 0.017 rad., compared to 0.09 rad for the side strengthened beams.

Acknowledgments

The work described has been realized with the co-operation of the RC Laboratory staff and Engineering majors J. Anastasakis and J. Kyriakides. The financial assistance of the Organization for Seismic Planning and Protection, is gratefully acknowledged.

References

- ACI Committee 440. 2000. Externally Bonded FRP Systems for Strengthening Concrete Structures (ACI 440-2R.02), American Concrete Institute, Farmington Hills, Michigan.
- Alagusundaramoorthy P., I. Harik and C. Choo. 2003. Flexural Behavior of RC Beams Strengthened With Carbon Fiber Reinforced Polymer Sheets of Fabric, *Jrnl. of Composites for Construction*, 7(4), 292-301.
- Bencardino F., Spadea G. and R. Swamy. 2002. Strength and Ductility of Reinforced Concrete Beams Externally Reinforced With Carbon Fiber Fabric, *ACI Structural Jrnl.*, 99(2), 163-171.
- Bonacci J. and M. Maalej. 2001. Behavioral Trends of RC Beams Strengthened With Externally Bonded FRP, *Jrnl. of Composites for Construction*, 5(2), 102-113.
- Bousselham A. and O. Chaallal. 2004. Shear Strengthening Reinforced Concrete Beams with Fiber – Reinforced Polymer: Assessment of Influencing Parameters and Required Research, *ACI Structural Jrnl.*, 101(2), 219-227.
- Chadwell C. and S. Mahin, *UCFYBER User's Manual*, Univ. of California, Berkeley, 2000.
- FIB-TG 9.3. 2001. *Design and Use of Externally Bonded Fiber Polymer Reinforcement (FRP EBR) for Reinforced Concrete Structures*, Bulletin 14, Switzerland.
- Grace N.F., Abdel-Sayed G. and W.F. Ragheb. 2002. Strengthening of Concrete Beams Using Innovative Ductile Fiber-Reinforced Polymer Fabric, *ACI Structural Jrnl.*, 99(5), 692-700.
- Grace N.F., W.F. Ragheb and G. Abdel-Sayed. 2003. Flexural and Shear Strengthening of Concrete Beams Using Triaxially Braided Ductile Fabric, *ACI Structural Jrnl.*, 100(6), 804-814.
- Mac Beton / Degussa Hellas SA. 2002. Product Specification and Application Instructions.
- Micelli F., Raghu A. and A. Nanni. 2002. Strengthening of Short Span Reinforced Concrete T Joists With Fiber Reinforced Plastic Composites, *Jrnl. of Composites for Construction*, 6(4), 264-271.
- Pellegrino C. and C. Modena. 2002. Fiber Reinforced Polymer Shear Strengthening of Reinforced Concrete Beams With Transverse Steel Reinforcement”, *Jrnl. of Composites for Construction*, 6(2), 104 -111.
- Stratford T. and C. Burgoyne. 2003. Shear analysis of concrete with brittle reinforcement, *Jrnl. of Composites for Construction*, 7(4), 323-330.

- Triantafillou Th. and C. Antonopoulos. 2000. Design of Concrete Flexural Members Strengthened in Shear With FRP, *Jrnl. of Composites for Construction*, 4(4), 198-205.
- Vougioukas E., C. Zeris and M. Kotsovos. 2005. Towards a Safe and Efficient Use of FRP for the Repair and Strengthening of Reinforced Concrete Structures, *ACI Structural Jrnl.*, 102(4), 525-34.
- Zeris C. 2004. Experimental Investigation of the Repair and Strengthening of RC Members Using FRPs. Volume 1: Repair and Strengthening of RC Columns Using FRP and Volume 2: Alternative Methods of Beam Strengthening Using FRP. *Final Report*. Org. of Seismic Planning and Protection (in Greek).